Electronic Supplementary Information

Enhanced Stability and Performance of Air-Processed Perovskite Solar Cells via Defect Passivation with Thiazole-Bridged Diketopyrrolopyrrole-Based π-Conjugated Polymer

Chih-Yu Chang*, Chun-Chieh Wang

Department of Materials Science and Engineering, National Taiwan University of Science and Technology, Taipei 10607, Taiwan (R.O.C.) (E-mail: cychang@gapps.ntust.edu.tw)

Table S1. Comparison of the characteristics of air-processed PeSCs previously reported as well as the present work.

Source	Relative humidity [%]	V_{oc} [volt]	J_{sc} [mA cm^{-2}]	FF [%]	PCE [%]
Reference 1	15-25	1.14	23.60	77.0	20.80
Reference 2	≈25	1.09	23.46	78.51	20.08
Reference 3	35 ± 5	1.05	19.01	72.60	14.55
Reference 4	40	1.11	23.37	71.05	18.38
Reference 5	40 ± 5	1.09	23.50	69.00	17.71
Reference 6	45	1.11	22.64	77.51	19.48
Reference 7	≈50	0.64	18.85	40.70	5.67
Reference 8	60	1.058	22.97	79.80	19.39
Reference 9	60	1.07	22.17	77.44	18.34
Reference 10	≈60	0.91	21.70	64.50	12.73
Reference 11	70	1.05	23.03	74.88	18.11
Reference 12	70 ± 10	1.00	22.36	66.60	15.56
Reference 13	72.2	0.95	21.10	75.00	15.12
This work	72 ± 3	1.09	21.90	80.39	19.19

Table S2. Summary of the photovoltaic properties of device A measured at different sweep directions.

Sweep direction	V_{oc} [volt]	J_{sc} [mA cm^{-2}]	FF [%]	PCE [%]
Forward	1.01	20.45	68.91	14.23
Reverse	1.01	20.66	79.54	16.58

Table S3. Summary of the photovoltaic properties of device B measured at different sweep directions.

Sweep direction	V_{oc} [volt]	J_{sc} [mA cm^{-2}]	FF [%]	PCE [%]
Forward	1.09	21.20	78.55	18.14
Reverse	1.09	21.17	80.77	18.64

Table S4. Summary of the photovoltaic properties of the devices with various TBAI-doped PTzDPPBTz thicknesses

TBAI-doped PTzDPPBTz thicknesses [nm]	V_{oc} [volt]	J_{sc} [mA cm^{-2}]	FF [%]	PCE [%]
20	1.09	22.28	83.59	20.30
45	1.09	21.54	80.80	18.97
80	1.09	20.57	76.88	17.23

Table S5. Summary of the photovoltaic properties of TBAI-doped PTzDPPBTz-based devices with different active areas.

Active area [cm^2]	V_{oc} [volt]	J_{sc} [mA cm^{-2}]	FF [%]	PCE [%]
0.12	1.09	22.28	83.59	20.30
1.2	1.09	20.89	77.03	17.53
5.04	1.09	20.79	71.41	16.18

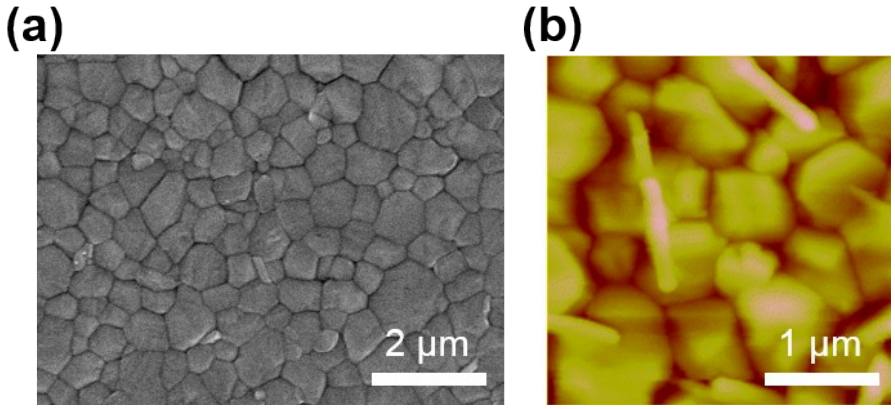

Fig. S1. Top view SEM image (left) and AFM topographic image (right) of $MAPbI_3$ film.

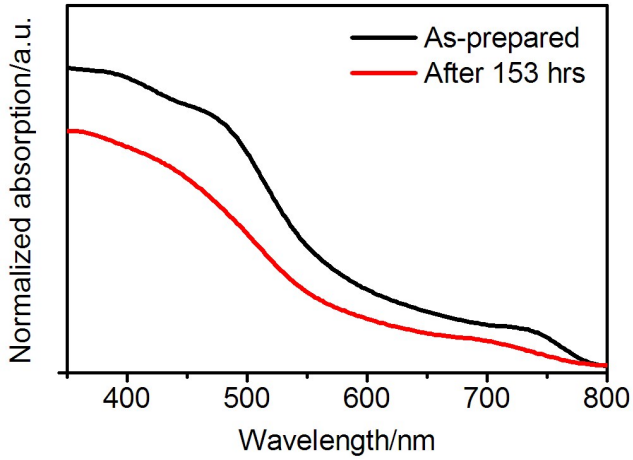

Fig. S2. Absorption spectra of $MAPbI_3$ perovskite film with PDPP passivation layer (the number-average molecular weight = 39 kDa) before and after being exposed to ambient air (25 °C and 60-70% relative humidity) for 153 hours.

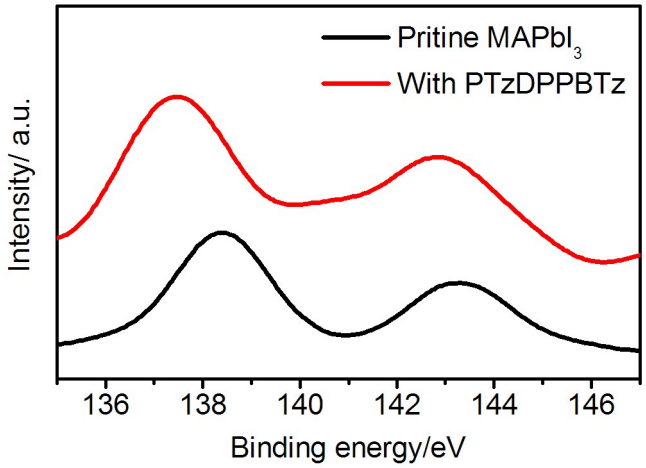

Fig. S3. XPS spectra of Pb 4f core level of $MAPbI_3$ film with and without PTzDPPBTz layer

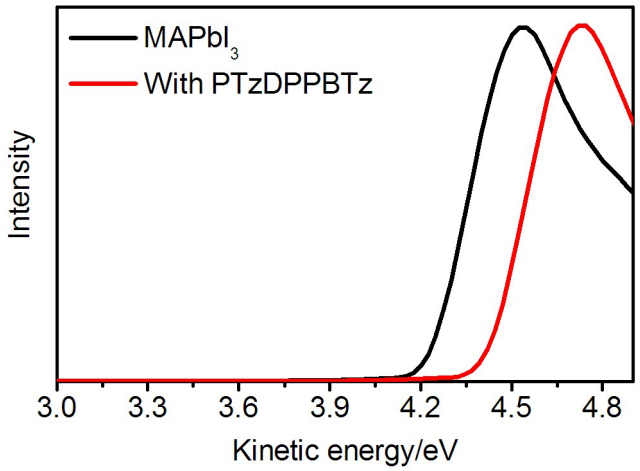

Fig. S4. UPS spectra of the secondary cutoff regions for perovskite film with and without PTzDPPBTz layer.

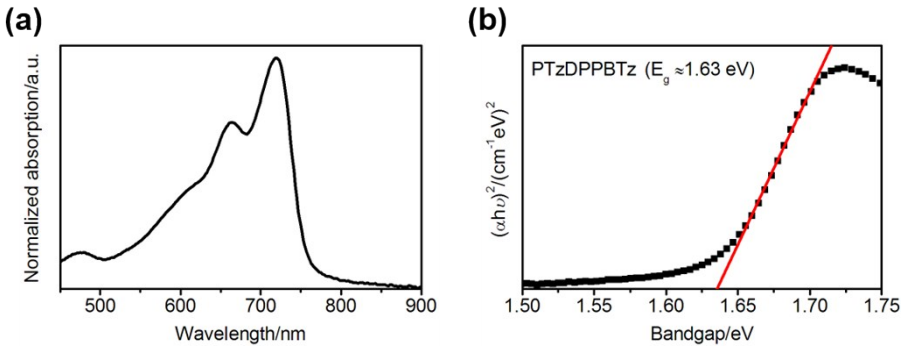

Fig. S5. (a) Absorption spectrum of PTzDPPBTz film. (b) Tauc plot of PTzDPPBTz film. The bandgap is determined by extrapolating the linear portion of the Tauc plot to the baseline.

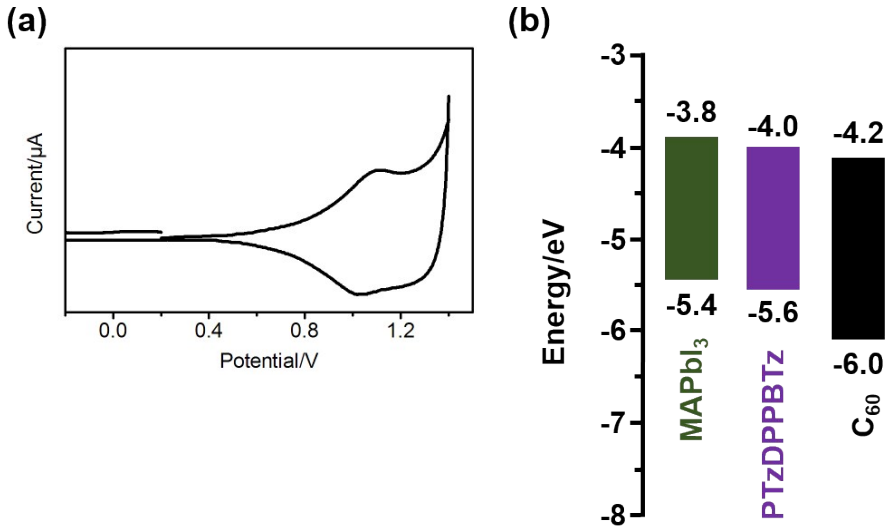

Fig. S6. (a) Cyclic voltammetry of PTzDPPBTz film. (b) Energy levels of the materials investigated in this study.

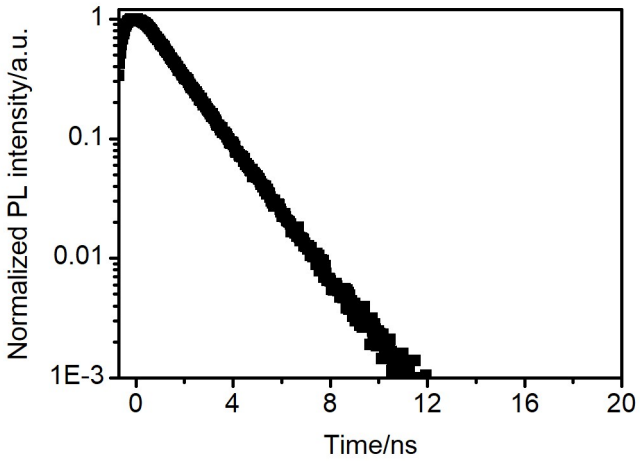

Fig. S7. Time-resolved PL spectrum of $MAPbI_3/C_{60}$ film.

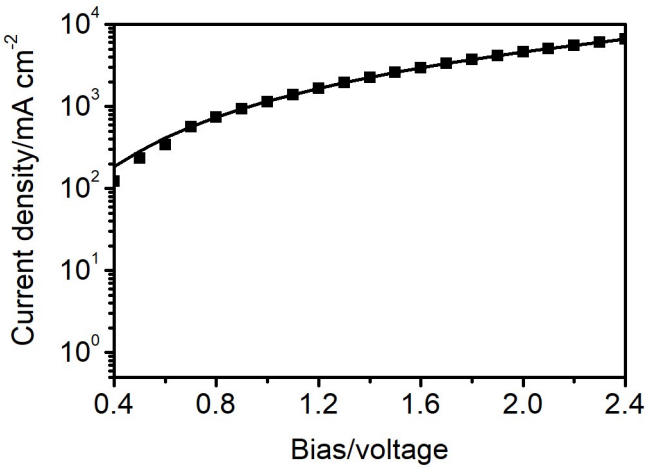

Fig. S8. Measured (symbol) and fitted (solid line) dark *J-V* characteristics for electron-only device (device structure: ITO-coated glass substrate/PEI/PTzDPPBTz/Ca/Al).

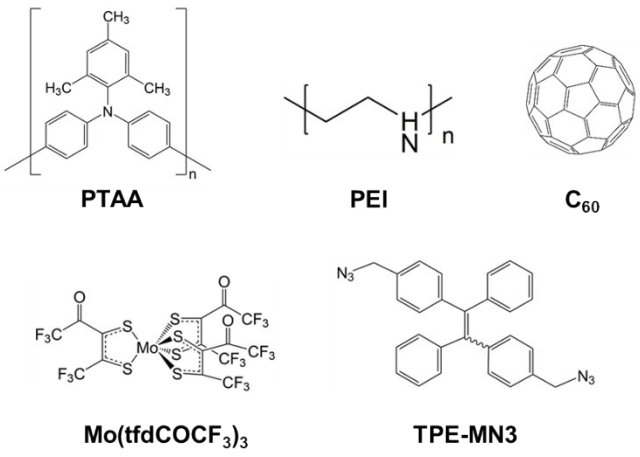

Fig. S9. Schematic illustration of the chemical structures of materials used in this study.

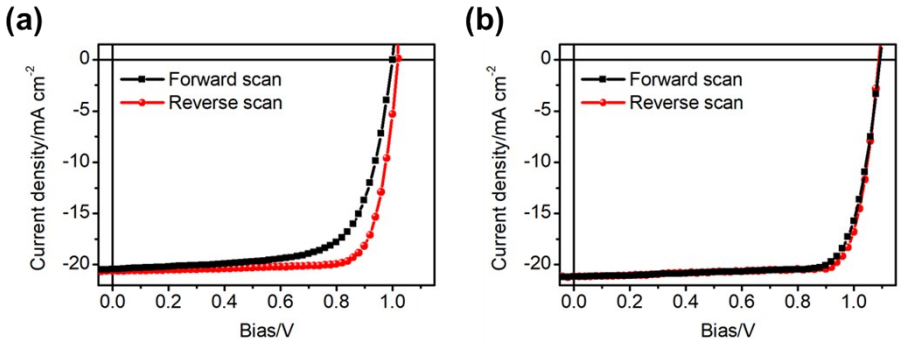

Fig. S10. *J-V* characteristics of the devices measured under simulated AM 1.5G solar irradiation (intensity = 100 mW cm^{-2}) with different sweep directions (scan rate = 0.15 V s^{-1}): (a) device A (see Table S2 for summary of photovoltaic characteristics of the device) and (b) device B (see Table S3 for summary of photovoltaic characteristics of the device).

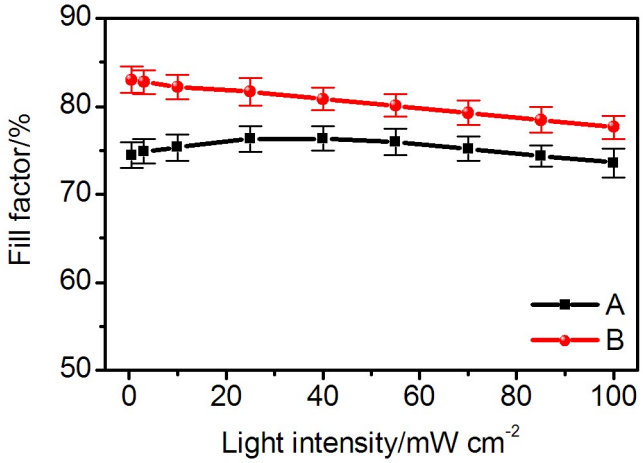

Fig. S11. Light intensity dependence of the fill factor of the devices; see Table 1 for descriptions of the device types. The statistical data were collected from more than 5 devices.

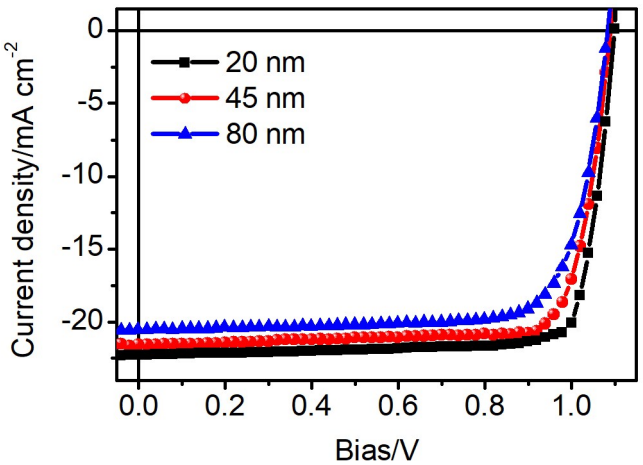

Fig. S12. *J-V* characteristics of the best-performing $MAPbI_3$-based devices with various n-doped PTzDPPBTz layer thicknesses (see Table S4 for summary of photovoltaic characteristics of the devices).

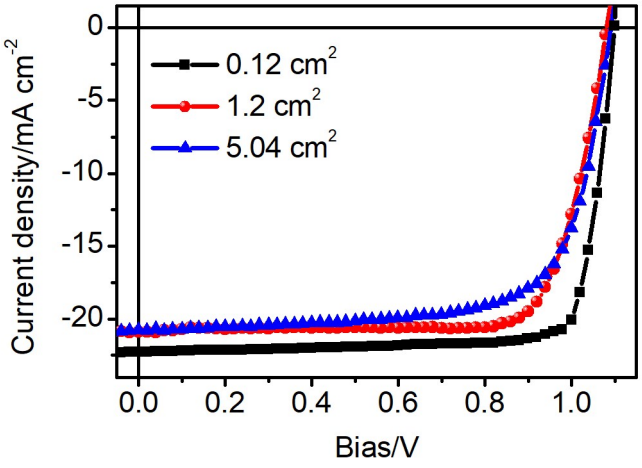

Fig. S13. *J-V* characteristics of the best-performing $MAPbI_3$-based devices with diifferent active areas (see Table S5 for summary of photovoltaic characteristics of the devices).

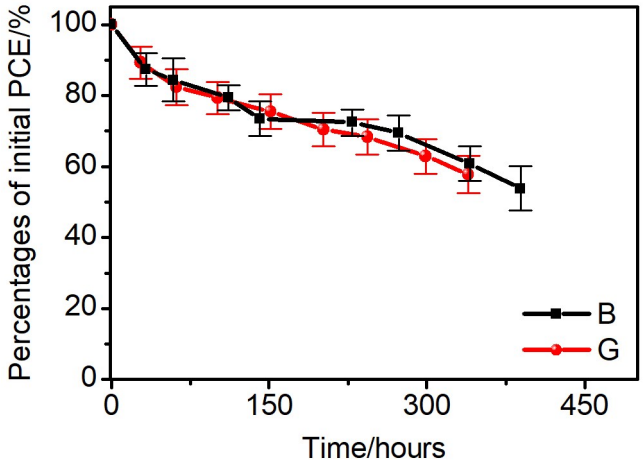

Fig. S14. Degradation profiles of the devices as a function of aging time under constant illumination (100 mW cm^{-2}) at their maximum power point in ambient conditions (25 °C and 70% relative humidity); see Table 1 and 2 for descriptions of the device types. The statistical data were collected from more than 5 devices.

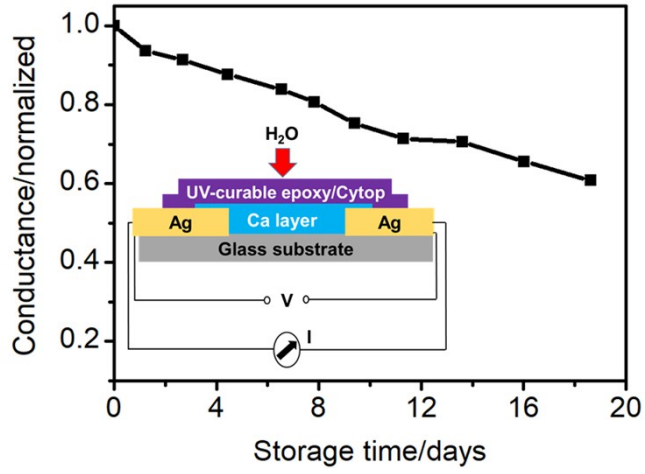

Fig. S15. Normalized conductance of Ca samples as a function of storage time in a controlled environment (25 °C and 70% relative humidity in air). Inset: structure of the device used for electrical Ca corrosion test.

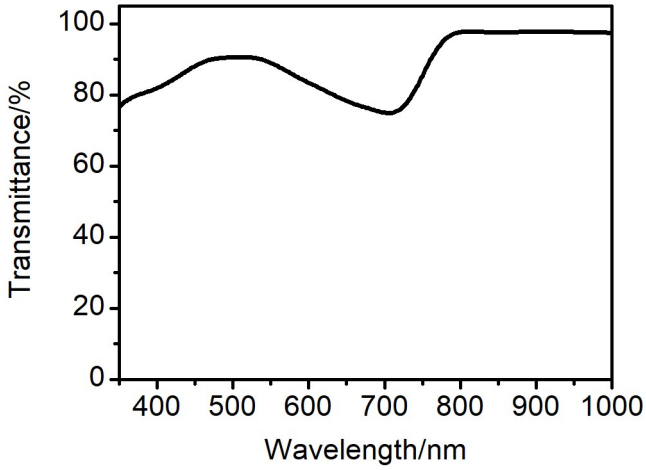

Fig. S16. Optical transmittance spectrum of ICL used herein.

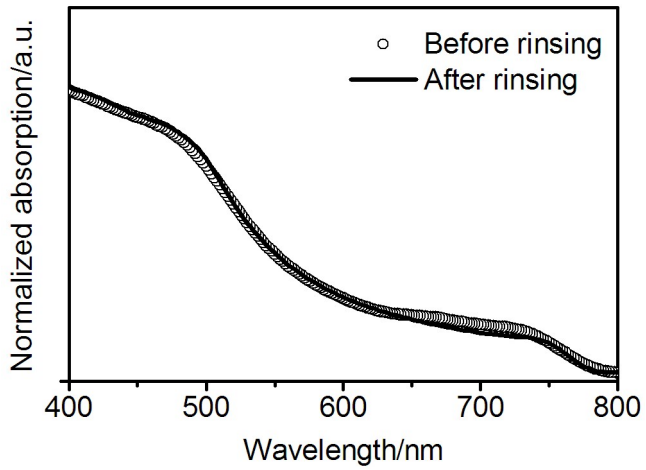

Fig. S17. Absorption spectra of ICL-coated $MAPbI_3$ film before and after rinsing with DMF.

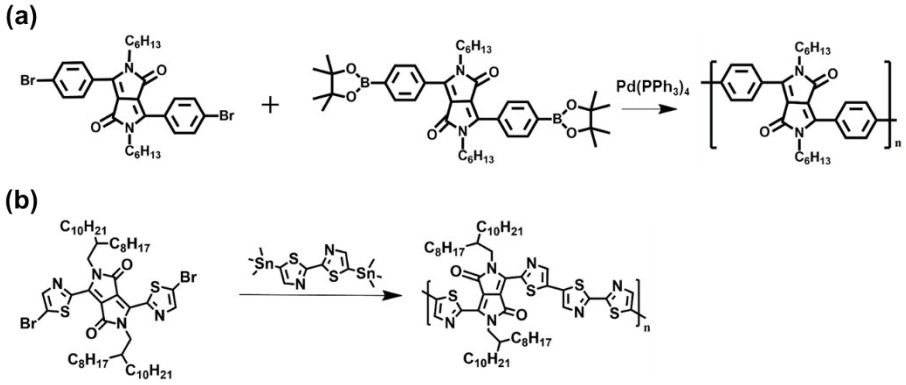

Fig. S18. (a) Synthetic scheme of PDPP. (b) Synthetic scheme of PTzDPPBTz.

References

1. T. Singh and T. Miyasaka, *Adv. Energy Mater.*, 2018, **8**, 1700677.
2. J. Ding, Q. Han, Q.-Q. Ge, D.-J. Xue, J.-Y. Ma, B.-Y. Zhao, Y.-X. Chen, J. Liu, D. B. Mitzi and J.-S. Hu, *Joule*, 2019, **3**, 402-416.
3. J. Huang, X. Yu, J. Xie, D. Xu, Z. Tang, C. Cui and D. Yang, *ACS Appl. Mater. Interfaces*, 2016, **8**, 21505-21511.
4. K. Huang, H. Li, C. Zhang, Y. Gao, T. Liu, J. Zhang, Y. Gao, Y. Peng, L. Ding and J. Yang, *Solar RRL*, 2019, **3**, 1800318.
5. L.-L. Gao, C.-X. Li, C.-J. Li and G.-J. Yang, *J. Mater. Chem. A*, 2017, **5**, 1548-1557.
6. C. Zuo, D. Vak, D. Angmo, L. Ding and M. Gao, *Nano Energy*, 2018, **46**, 185-192.
7. M. Seetharaman S, P. Nagarjuna, P. N. Kumar, S. P. Singh, M. Deepa and M. A. G. Namboothiry, *Phys. Chem. Chem. Phys.*, 2014, **16**, 24691-24696.
8. R. Cheng, C.-C. Chung, H. Zhang, Z. Zhou, P. Zhai, Y.-T. Huang, H. Lee and S.-P. Feng, *Small*, 2019, **15**, 1804465.
9. W.-T. Wang, J. Sharma, J.-W. Chen, C.-H. Kao, S.-Y. Chen, C.-H. Chen, Y.-C. Feng and Y. Tai, *Nano Energy*, 2018, **49**, 109-116.
10. P. Luo, Z. Liu, W. Xia, C. Yuan, J. Cheng and Y. Lu, *ACS Appl. Mater. Interfaces*, 2015, **7**, 2708-2714.
11. Y. Cheng, X. Xu, Y. Xie, H.-W. Li, J. Qing, C. Ma, C.-S. Lee, F. So and S.-W. Tsang, *Solar RRL*, 2017, **1**, 1700097.
12. X. Xu, C. Ma, Y.-M. Xie, Y. Cheng, Y. Tian, M. Li, Y. Ma, C.-S. Lee and S.-W. Tsang, *J. Mater. Chem. A*, 2018, **6**, 7731-7740.
13. Q. Tai, P. You, H. Sang, Z. Liu, C. Hu, H. L. W. Chan and F. Yan, *Nat. Commun.*, 2016, **7**, 11105.